Small-angle X-ray scattering studies of crystallization in crosslinked linear polyethylene*

W. Scott Lambert† and Paul J. Phillips‡
Department of Materials Science and Engineering, University of Tennessee, Knoxville, TN 37996-2200, USA

and J. S. Lin
Center for Small Angle Scattering Research, Oak Ridge National Laboratories, Oak Ridge, TN 37831, USA
(Received 18 May 1993; revised 20 July 1993)

The results of a comprehensive small-angle X-ray scattering study of linear polyethylene crosslinked using a peroxide have been combined with a study of the crystallization kinetics to obtain a generalized picture of the effects of limited mobility and comonomer content on crystallization. It is shown that there are three regions of behaviour: (i) an initial region in which the crosslinks are soluble in the crystal to a certain limiting composition; (ii) a region in which the lamellar thickness decreases in a continuous manner with increasing crosslink density; and (iii) a region where the lamellar thickness is virtually independent of crosslink density. The results are interpreted using the Sanchez–Eby theory, the Andrews theory and regime theory to generate a comprehensive description of the behaviour.

(Keywords: small-angle X-ray scattering; linear polyethylene; crystallization kinetics)

INTRODUCTION

The crosslinking of a polymer influences crystallization in three clearly different ways. First, it eliminates reptation in its conventional sense, only 'reptation slack' being available for movements of the polymer chains over distances exceeding nanometres. Secondly, the need for exclusion of the bulky crosslinks significantly reduces the rate of secondary nucleation in a way which results in the growth rate decreasing exponentially with crosslink density. Thirdly, the presence of excluded defects in the form of crosslinks controls the upper limit possible for lamellar thickness. The first of these effects is unique to crosslinking, whereas the remaining two effects are to be found in all copolymers having excludable comonomer units. Insights obtained from the study of the effects of crosslinking, other than the reptation effects, are therefore of general significance to the study of copolymers. In many ways the use of crosslinking as a means of studying copolymers generates a range of model systems with greater flexibility than is possible with commercially available copolymers. Crosslinking of well characterized polyolefins can be achieved easily through the use of an appropriate peroxide and hence generates a series of 'copolymers' that differ only in terms of the comonomer content. An additional advantage is that molecular weight effects are suppressed as the polymers are all of infinite molecular weight.

In earlier publications[1,2], we have reported the effects of increasing crosslink density on the crystallinity, unit cell parameters, melting behaviour[1] and crystallization kinetics[2] of linear polyethylene crosslinked using Vulcup-R©. It was demonstrated that the initial introduction of crosslinks caused the established regime I–regime II[3] behaviour of linear polyethylene to change to regime III[4,5]. This was attributed to the loss of reptational ability, drastically reducing the rate of surface spreading g relative to the rate of secondary nucleation i. As crosslink density was increased, the overall rate of crystallization dropped in a continuous manner due to a reduction in the rate of secondary nucleation i via the copolymer exclusion effect[6]. The kinetic data were analysed using the Andrews theory[6], in which the logarithm of the isothermal growth rate was plotted against the concentration of excluded units. A straight-line fit was applied and the slope yielded an estimate of the critical nucleus size as a length of continuous chain approximately equal to three stem lengths[2] using an assumed value of the lamellar thickness. There was considerable scatter in that plot and additional formulations have now been considered in order to construct a more reliable interpretation. The use of actual lamellar thicknesses in the calculations is now possible.

In all studies of crystallization, the determination of the dependence of lamellar thickness on temperature, pressure and other parameters has played a major part in developing a fundamental understanding of the process. Such investigations have been a major deficiency in our earlier studies, which has now been rectified. It will be shown that the dependence of lamellar thickness

* Presented at 'International Polymer Physics Symposium Honouring Professor John D. Hoffman's 70th Birthday', 15–16 May 1993, Washington, DC, USA
† Present address: Cryovac Division, WR Grace Co., Duncan, SC, USA
‡ To whom correspondence should be addressed

0032-3861/94/09/1809–10

Table 1 Characterization data of crosslinked PEs

Vulcup-R (wt%)	Extractables (%)	Molecular weight between crosslinks ($\times 10^{-3}$)	Average number of methylene units
0.1	17.9	17.3	1238
0.3	16.5	12.7	907
0.4	12.5	9.4	669
0.5	8.3	5.7	410
0.7	8.8	4.5	324
0.9	5.5	3.6	255
1.2	4.5	3.1	219
1.5	3.8	2.2	155
2.5	3.6	1.9	136
3.1	2.9	1.3	95
4.2	3.9	0.96	68
5.0	4.5	0.56	40

on crosslink density generates considerable insight into the phenomenology of the general influence of essentially excludable comonomer units on crystallization, which has hitherto been lacking.

EXPERIMENTAL

Linear polyethylene (PE) was crosslinked and characterized as previously described[1,7]. Additional specimen loadings were considered in this study, the results of the characterizations of all of the crosslinked polyethylenes being given in *Table 1*.

Small-angle X-ray scattering (SAXS) studies were carried out at the Center for Small Angle Scattering Research (CSASR) at the Oak Ridge National Laboratories on their 10 m SAXS camera. The scattering system has been fully described by Hendricks[8] and Lee[9]. Scattering was carried out both at room temperature and at the crystallization temperatures (*in situ*). Samples were first isothermally crystallized and then quenched to room temperature. Samples analysed at the crystallization temperature (*in situ*) were mounted in a cell surrounded by copper tubing. A temperature control bath was attached to the copper tubing in the X-ray sample chamber and hot ethylene glycol was circulated around the sample. The temperature was monitored using a thermocouple which was in contact with the sample. This allowed the temperature of the sample to be raised from room temperature to the crystallization temperature in a controlled manner. Crystallization kinetics studies were carried out for the additional samples using the procedures detailed earlier[2].

RESULTS

The crystallinities of the isothermally crystallized samples were calculated using wide-angle X-ray diffraction (WAXD) data. The crystalline diffraction peaks were separated from the amorphous halo by drawing a line connecting the minima between the crystalline peaks. The diffraction pattern was then separated into three areas corresponding to the amorphous area and (110) and (200) peak areas. The combined correction factors for the amorphous, (110) and (200) peaks are 0.69, 1.00 and 1.43, respectively. The crystallinity is then expressed by the relation

$$W_c = 100 \times \frac{I_{110} + 1.43 I_{200}}{I_{110} + 1.43 I_{200} + 0.69 I_A}$$

Table 2 shows the crystallinities of the gel fractions, which are seen to increase slightly up to intermediate crystallization temperatures and then to decrease at higher crystallization temperatures. Crystallinities decrease for specimens beyond G-0.5 as the crosslink densities of the systems are increased.

SAXS data were initially collected in the form of scattering intensity contour plots. All SAXS patterns were found to be circularly symmetrical, indicating the absence of orientation in the compression-moulded films. The isointensity contour plots were then radially averaged to obtain one-dimensional intensity plots as a function of the scattering vector q. Typical scattering intensity *versus* scattering vector curves obtained at room temperature are shown in *Figures 1* to *4* for original polyethylene (OPE), G-0.1, G-1.5, and G-5.0, respectively. Typical curves obtained *in situ* are shown for G-0.1, G-1.5 and G-5.0 in *Figures 5* to *7*, respectively. It can be seen that the maximum in the intensity shifts to higher values of q upon initial crosslinking, as shown in *Figures 1* and *2*, and upon additional crosslinking, as demonstrated in *Figures 3* and *4*.

From the peaks in the Lorentz-corrected intensity *versus* scattering vector plots, it is possible to calculate the long periods and lamellar thicknesses of the gel fractions. The long period may be calculated from the Bragg law by determining the scattering angle corresponding to the maximum in the scattering intensity. The crystallinity values given in *Table 2* were used to calculate the lamellar thicknesses of the crosslinked systems assuming a two-phase, semicrystalline model. *Table 3* gives the results for the long period and lamellar thickness calculations. OPE, G-0.1 and G-0.3 show a slight increase in lamellar thickness with increasing crystallization temperature, while samples of higher crosslink density show no variation with crystallization temperature. The results for the long periods and lamellar thicknesses determined *in situ* are given in *Table 4*, and they show a similar variation to those determined at room temperature. The values in *Table 3* are similar to those in *Table 4* except at the highest temperatures, suggesting that the long period of the system is controlled by the long period of the crystal which is most prevalent in the material.

DISCUSSION

The lamellar thickness results in *Tables 3* and *4* show that crystallization temperature has little effect on lamellar thickness. In these systems, however, crosslink density has a clear effect. *Figure 8* shows the variation in lamellar thickness with defect content of the gel fractions determined at room temperature. A similar plot can be seen in *Figure 9* for the SAXS results obtained at the crystallization temperature. The defect content was calculated as the reciprocal of the chain length between crosslinks. The data shown include two different temperatures since it is impossible to find a common crystallization temperature for all of the gel fractions. *Figures 8* and *9* are divided into three regions, A, B and C.

In region A, lamellar thickness increases slightly with increasing defect content. This suggests that at low impurity contents, crosslinks may be incorporated into the crystals. Such behaviour could explain the initial upsurge in the crystallinity with defect content. The incorporation of defects into crystals has been considered in the work of Sanchez and Eby[10,11]. The crosslink in

Table 2 Crystallinities (%) of isothermally crystallized gel fractions measured at room temperature

Crystallization temperature (°C)	OPE	G-0.1	G-0.3	G-0.4	G-0.5	G-0.7	G-0.9	G-1.2	G-1.5	G-2.5	G-3.1	G-4.2	G-5.0
97													39.5
99												47.6	50.6
101											52.6	49.7	49.3
102												49.2	51.0
103											51.6	49.2	45.7
104												45.0	45.8
105										54.6	47.7	47.2	47.2
106											50.9	44.9	47.8
107									57.2	60.6	50.5	43.3	43.7
108											51.1	44.4	43.7
109							60.6	58.7	56.7	55.8	53.6	41.0	45.9
110									54.3	58.5	46.9		
111						57.3	56.2	61.2	58.4	55.1	58.9		
112						59.2	59.6	57.7	56.1	55.1	48.6		
113		52.8	58.1	61.3	60.2	59.8	54.7	55.8	57.5	54.2			
114				58.9	61.9	58.2	63.2	58.0	55.3	54.2			
115		60.7	62.4	62.1	61.9	56.9	57.1	60.3	57.3	56.3			
116		64.3	66.3	64.7	61.7	59.6	59.2	56.0	51.2	59.2			
117		66.7	64.1	58.8	56.0	63.9	53.9	52.2	55.5	43.7			
118		60.3	66.4	58.3	62.9	57.5	64.2	60.4					
119	64.2	63.1	66.4	60.0	60.4	60.7	58.7	52.3					
120	67.6	61.1	63.2	59.0	65.6	55.9							
121		63.7	62.6	52.4	61.6	55.6							
122	67.5												
123	69.7												
124													
125	72.6												
126	72.8												
127	69.1												

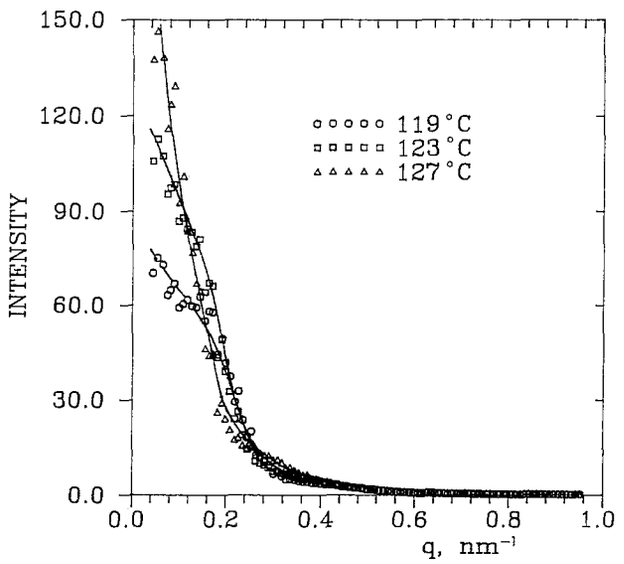

Figure 1 SAXS curves for OPE at room temperature as a function of crystallization temperature

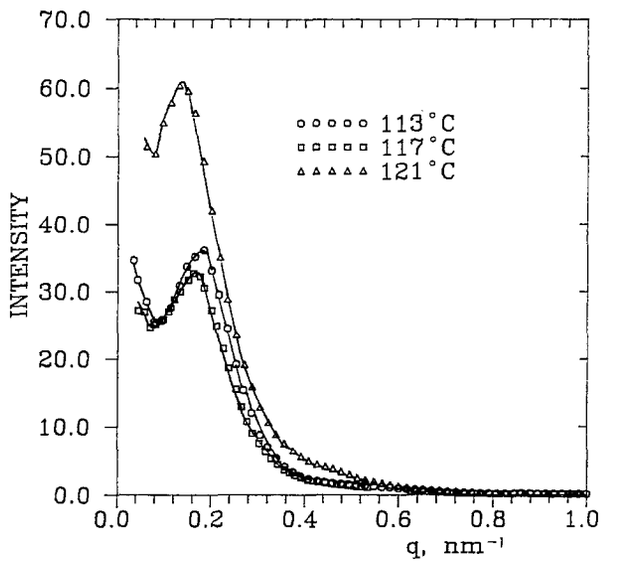

Figure 2 SAXS curves of G-0.1 at room temperature as a function of crystallization temperature

crosslinked polyethylene (XLPE) that has been crosslinked using a peroxide consists simply of a carbon–carbon bond replacing two hydrogen atoms. As such it occupies a lower volume than the species replaced (see *Figure 10*). Provided that the four arms of the crosslink are able to align as shown in *Figure 10*, incorporation into the crystal should not be difficult. As suggested by Sanchez and Eby[10,11], the incorporation of comonomer units (in this case crosslinks) into the crystal will reduce the enthalpy of fusion. In turn this reduction in the enthalpy will cause

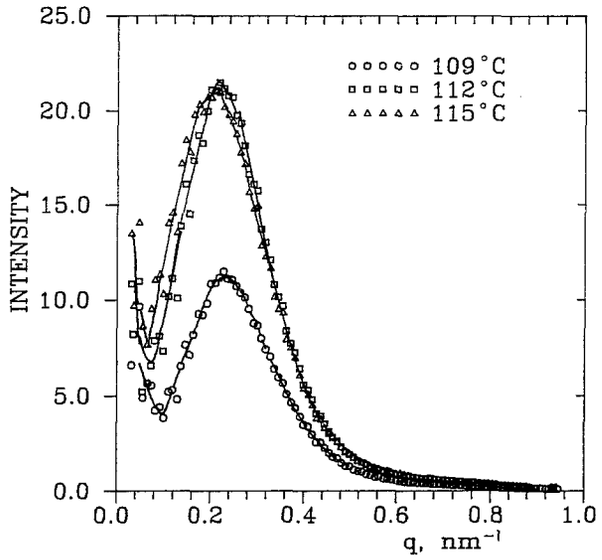

Figure 3 SAXS curves of G-1.5 at room temperature as a function of crystallization temperature

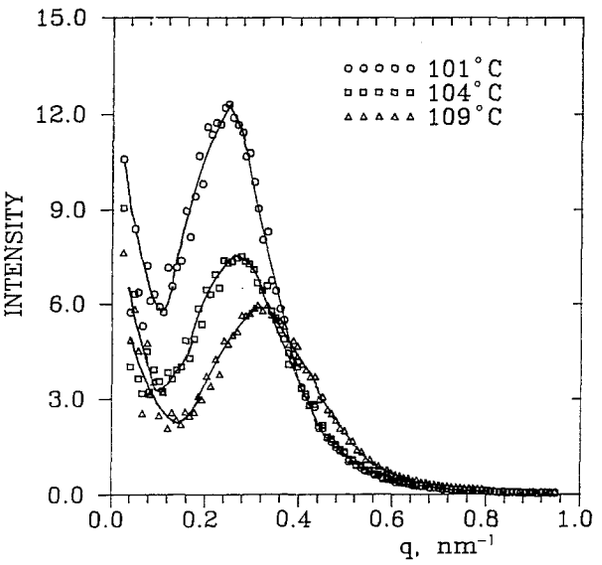

Figure 4 SAXS curves of G-5.0 at room temperature as a function of crystallization temperature

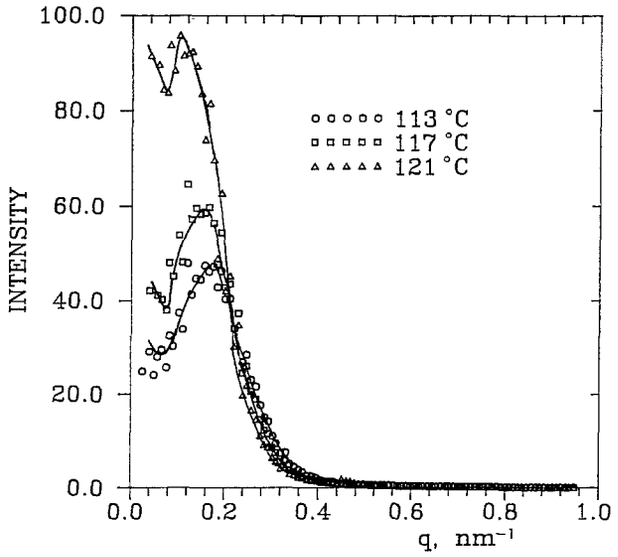

Figure 5 SAXS curves of G-0.1 measured at the crystallization temperatures indicated

an increase in lamellar thickness, if all other parameters, such as fold surface free energy, remain unchanged. It is anticipated that there will be a solubility limit for the crosslinks in the crystal, as in most substitutional solid solutions. In this case the solubility limit lies between 579 and 907 methylenes between crosslinks, or between 0.1 and 0.2% defects. The specific case of incorporation of this type of crosslink into a polyethylene was considered using elasticity theory by Guiu and Shadrake[12], who calculated the lattice distortions. They concluded that the lattice strains were tolerable, but they did not estimate a solubility limit.

It is appropriate to apply the Sanchez–Eby theory[10,11] to the results for region A. Although there are only two points available, the approach is justified since there is a paucity of such calculations in the literature. This is largely a result of most copolymer systems being of the defect exclusion type. The slope of the initial section has been calculated as 7×10^{-5} cm using the points at 177 Å for 1238 methylenes between crosslinks, or a

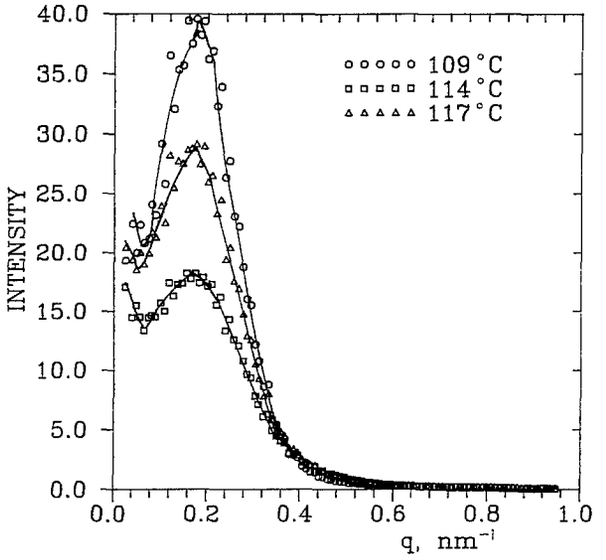

Figure 6 SAXS curves of G-1.5 measured at the crystallization temperatures indicated

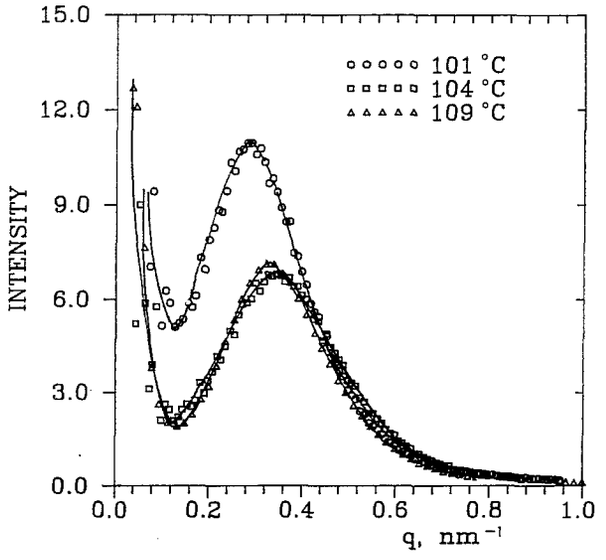

Figure 7 SAXS curves of G-5.0 measured at the crystallization temperatures indicated

Table 3 Lorentz-corrected SAXS data of isothermally crystallized gel fractions measured at room temperature

Crystallization temperature (°C)	Long period (Å)	Lamellar thickness (Å)	Height ratio	Distance ratio
OPE				
119	330	212		
120	330	223		
121	370			
122	370	248		
123	370	256		
124	370			
125	370	266		
126	370	267		
127	436	302		
G-0.1				
113	291	154	0.70	2.33
115	291	177	0.63	2.09
116	297	191	0.60	2.47
117	297	198	0.75	2.27
118	312	188	0.98	1.36
119	314	198	0.77	1.88
120	297	181	0.92	1.70
121	313	199	0.83	1.65
G-0.3				
113	267	155	0.68	2.33
115	291	181	0.66	2.33
116	297	197	0.59	2.47
117	297	190	0.78	1.96
118	297	197	0.73	2.27
119	314	209	0.69	3.44
120	297	197	0.97	1.23
121	313	181	0.89	1.65
G-0.4				
113	289	177	0.63	2.65
114	289	170	0.67	2.35
115	289	179	0.58	1.98
116	278	180	0.81	2.04
117	289	170	0.63	2.21
118	289	168	0.76	1.98
119	289	173	0.72	1.98
120	278	164	0.85	1.63
121	278	146	0.97	1.08
G-5.0				
97	184	82	0.28	2.50
99	169	85	0.40	2.28
101	176	87	0.33	2.37
102	158	80	0.47	2.28
103	161	74	0.29	2.83
104	145	66	0.30	2.71
105	144	73	0.23	2.83
106	160	76	0.31	2.70
107	141	62	0.24	2.98
108	160	70	0.33	2.35
109	161	74	0.27	2.44

1.5×10^{-3} mole fraction, and 181 Å for 907 methylenes between crosslinks, or a 2.1×10^{-3} mole fraction.

Using the equation

$$\text{slope} = A \frac{2\sigma_e}{\Delta H_f} \left(\frac{T_m^\circ}{T_m^\circ - T} \right)^2$$

and values[13] of $\sigma_e = 93\ \text{erg cm}^{-2}$ and $\Delta H_f = 2.8 \times 10^9\ \text{erg cm}^{-3}$, the value of A was calculated to be 3.5, and this corresponds to the ratio of the excess free energy of the defect (E) to the heat of fusion (ΔH_f). Calculation of E/RT shows it to be 0.29. Sanchez and Eby found A to be 1.4 for random copolymers of tetrafluoroethylene and hexafluoropropylene[10] and 0.43 for copolymers of D- and D-, L-lactides crystallized from solution[11]. The high values of A and E/RT for the system being studied here suggest that it is primarily a defect exclusion system. This is borne out by the low solubility limit of the crosslinks in the crystal, as demonstrated by the downturn in the lamellar

Table 4 Lorentz-corrected SAXS data of isothermally crystallized gel fractions measured *in situ* at the crystallization temperature

Crystallization temperature (°C)	Long period (Å)	Lamellar thickness (Å)	Height ratio	Distance ratio
G-0.1				
113	274	145	0.54	2.32
115	274	167	0.67	1.82
117	274	183	0.64	2.19
119	298	188	0.65	1.95
121	327	208	0.91	1.70
G-0.4				
113	274	168	0.61	2.67
115	274	170	0.60	2.08
116	274	178	0.68	2.32
117	274	161	0.62	2.39
120	298	176	0.73	1.82
121	327	171	0.87	1.55
G-0.7				
112	274	144	0.48	3.59
113	274	164	0.63	2.32
115	274	156	0.61	3.21
117	274	175	0.57	3.59
118	274	158	0.62	2.32
120	327	183	0.82	1.82
121	327	182	0.84	1.82
G-1.5				
107	213	108	0.30	4.36
109	274	156	0.51	3.59
111	254	148	0.41	3.76
114	254	140	0.73	2.39
115	214	122	0.50	3.20
116	214	109	0.74	2.57
117	274	152	0.64	3.59
G-3.1				
101	190	100	0.24	3.76
103	190	98	0.37	2.31
105	190	90	0.33	2.25
107	213	108	0.30	4.36
109	213	105	0.39	3.76
111	213	109	0.40	3.55

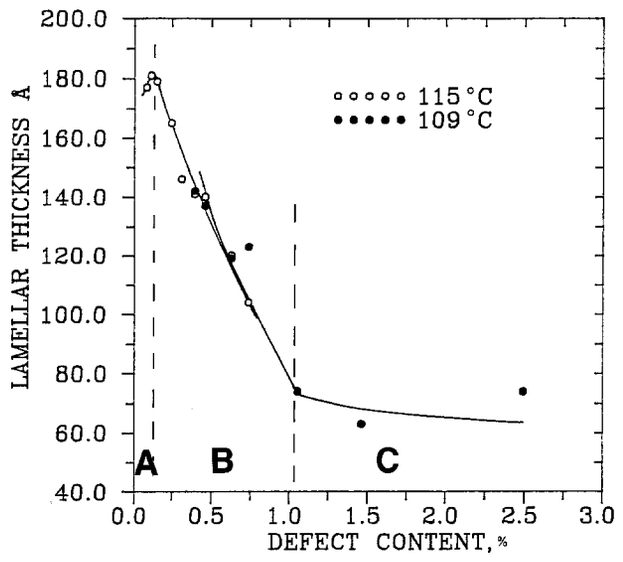

Figure 8 Lamellar thickness of the gel fractions at room temperature as a function of defect content for crystallization at 115°C and 109°C

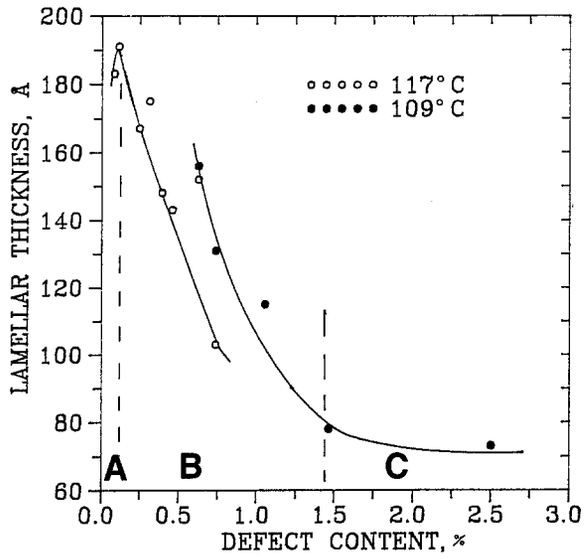

Figure 9 Lamellar thickness of the gel fraction at the crystallization temperatures of 117°C and 109°C as a function of defect content

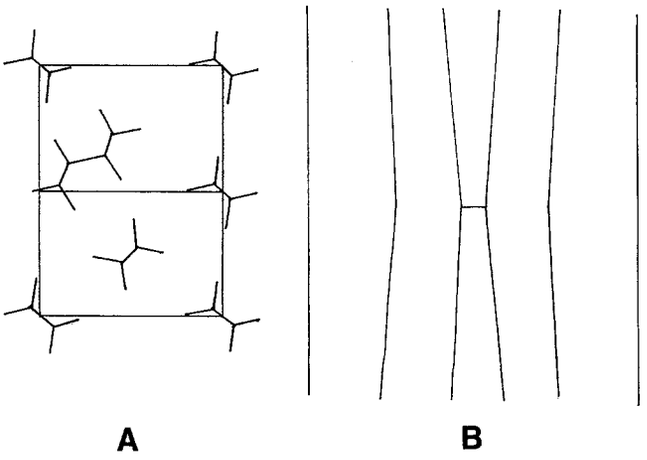

Figure 10 Schematic diagram of the incorporation of carbon–carbon crosslinks into the polyethylene crystal: (A) (0 0 1) plane; (B) (1 1 0) plane

thickness in region B. Overall, this turn of events is not particularly surprising given the fact that a crosslink ties together two stems, whereas in strictly random copolymers the defect affects only one stem. The effect of the crosslink defect should therefore be much larger than that of a typical comonomer defect.

In region B, the lamellar thickness decreases with increasing crosslink density due to the decrease in chain length between crosslinks. Assuming that the crystal is defect free or that a constant solubility limit applies, then as the chain length between defects decreases, the lamellar thickness will also decrease. This behaviour is in apparent contradiction to the random copolymer theories of inclusion (Flory[14]) and exclusion (Sanchez–Eby[10,11]) as, according to Sanchez and Eby, both theories predict that the lamellar thickness should increase with comonomer content for thermodynamic reasons. However, this does not take into account the physical limit on lamellar thickness dictated by sequence lengths in the exclusion case. Also, the thickening coefficient (γ) must be dependent on sequence length and hence cannot be a constant for the exclusion case.

In region C, the lamellar thickness levels off with increasing defect content. The decrease in region C is not as drastic as that in region B. Samples in region C have chain lengths between crosslinks that are similar to the lamellar thickness, suggesting that only single stems are laid down during crystallization. The data in *Table 5* support this conclusion. The maximum number of stems was calculated by dividing the average chain length between crosslinks by the stem length and does not take into account chain lengths used in folds, interlamellar links, or amorphous material. The stem lengths in *Table 5* were calculated from the thinnest lamellae measured for each sample assuming a 30° tilt angle[15], hence the number of stems listed is the maximum number that can be formed. The stem length in region C is directly controlled by the chain length between crosslinks. Gielenz and Jungnickel[16] and Jäger *et al.*[17] have reported similar results for radiation-crosslinked polyethylene. They have shown that for defect contents less than 1%, the polyethylene crystallizes in a chain-folded manner, and for defect contents greater than 1%, the polyethylene crystallizes by the laying down of single stems.

Our earlier works[1,2,7] have discussed the effects of crosslinking on crystallization in polyethylene. It was found that the introduction of crosslinks into linear polyethylene results in a reduction in the rate of crystallization, as noted by the leftwards shift of the curves in *Figure 11*. The data presented in *Figure 11* comprise all of those originally reported[2], together with those of the additional formulations prepared for this study. The half-time data have been processed as described earlier to produce the secondary nucleation plots shown in *Figure 12*. It is noted that the switch from regime I–regime II to regime III on initial crosslinking has been retained. This phenomenon is ascribed to a severe reduction in the rate of lateral spreading caused by the inability of the chain to reptate. The loss of reptational ability is caused by a lack of chain ends in the material. This reduction in the rate of lateral spreading permits the rate of secondary nucleation to dominate, resulting in regime III growth.

The data for the lowest three crosslink density materials (400–900 methylenes between crosslinks) are indistinguishable from one another. It will be recalled that this behaviour could not be explained in an earlier report[2]. This range of crosslinked densities corresponds to the range that showed an increasing lamellar thickness

Table 5 Lamellar characteristics and thickening coefficients of gel fractions

Sample	Chain length between crosslinks (Å)	Stem length[a]	Maximum number of stems	Thickening coefficient γ
OPE				3.48
G-0.1	1572	167	9.4	2.06
G-0.3	1152	179	6.5	2.19
G-0.4	850	189	4.5	1.83
G-0.5	521	191	2.8	1.90
G-0.7	412	170	2.5	1.59
G-0.9	324	148	2.2	1.70
G-1.2	278	125	2.3	1.68
G-1.5	197	100	2.0	
G-2.5	173	97	1.8	1.56
G-3.1	121	104	1.2	1.53
G-4.2	86	71	1.2	3.60
G-5.0	51	71	0.7	3.24

[a] Assuming a 30° tilt angle[15]

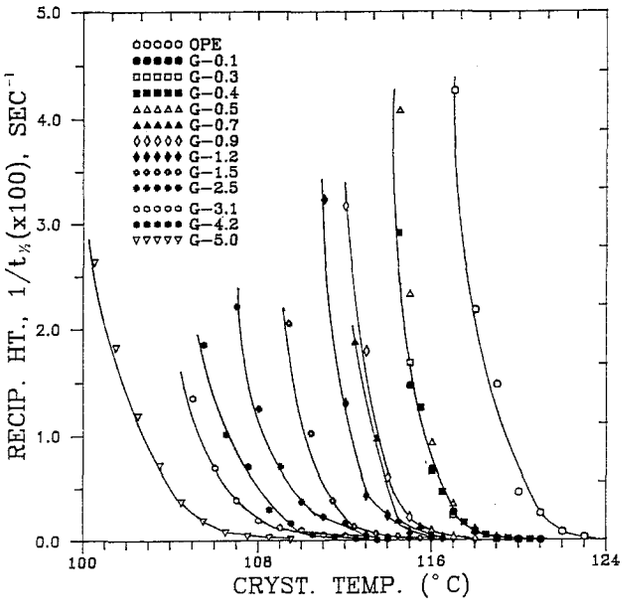

Figure 11 Reciprocal half-times for the bulk crystallization of the gel fractions as a function of crystallization temperature

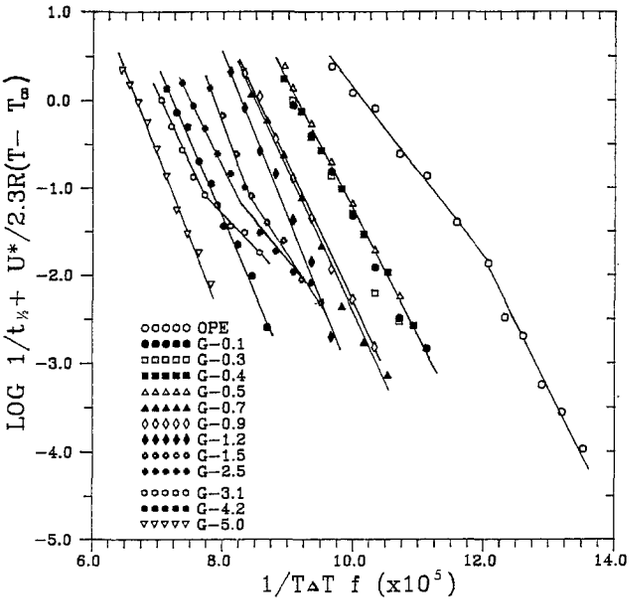

Figure 12 Secondary nucleation analyses of the bulk growth kinetics of the gel fractions assuming heterogeneous nucleation

with crosslink density, ascribed to the solubility of crosslinks in the crystal and an ensuing increase in crystallinity.

In an earlier report[2] it was noted that a regime II–regime III transition appeared for the highest crosslink densities. The range of specimens available has been extended with unexpected results being encountered. It can now be concluded that the regime II–regime III region is characteristic of polymers with 95–155 methylene groups between crosslinks. This behaviour was, and still is, attributed to the reduction in the rate of secondary nucleation caused by the copolymer effect. In other words, the rate of secondary nucleation was reduced so much by the microstructural defects that it became comparable to the rate of lateral spreading. For these specimens where the maximum number of stems possible between crosslinks is low, it must be recognized that the rate of lateral spreading will be determined by the deposition of stems from nearby sections of chain and not by an adjacent re-entry process. The two highest crosslink density materials (40 and 68 methylenes between crosslinks) show only regime III crystallization. It is remarkable that the rate of growth for G-4.2 (68 methylenes) is greater than that for G-3.1 (95 methylenes) for the temperature region over which both show regime III growth. It was noted earlier in this paper that the lamellar thicknesses for these two highest crosslink densities were comparable to the average sequence lengths between crosslinks. This observation suggests that there has been a switch from the three-stem nucleus[2,18] to a single-stem nucleus in G-4.2 and G-5.0. This would account for the increase in growth rate on population grounds as single-stem nuclei would be much more plentiful than three-stem nuclei. When applied to a partition function calculation the population numbers effect would overwhelm the higher energy of critical nucleus formation effect and give an increase in the rate of secondary nucleation.

In an earlier report[2] further analyses using the theory of Andrews *et al.*[6] showed the critical nucleus to consist of three stems based on an assumed lamellar thickness of 120–150 Å. Originally, a single linear fit was applied over the full range of growth data in the Andrews analysis because of the limited growth data available. Reciprocal half-times were used in place of linear growth rates, with data taken only from regime III. Additional specimens have been prepared in the interim, and more data points obtained, the complete data set being shown in *Figure 11*. The new Andrews plot is shown in *Figure 13*, where it can be seen that the data have a similar shape to that of the SAXS data shown in *Figures 8* and *9*. Straight-line fits have been applied to limited ranges of defect contents corresponding to the three regions of the lamellar thickness data. As explained earlier, at low defect contents (0.2%) crosslinks are incorporated into the crystals, this being reflected in the initial increase in both the lamellar thicknesses and the growth rate data. At defect contents greater than 0.2%, the lamellar thickness is controlled directly by the chain length between defects. Therefore,

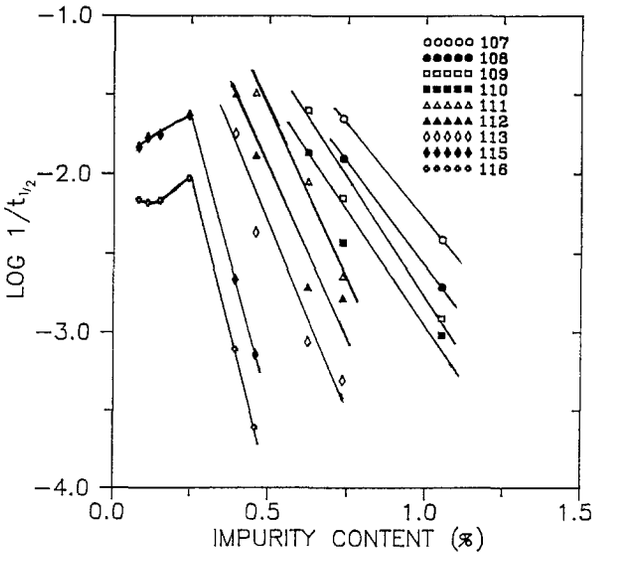

Figure 13 Analysis of gel fraction kinetics at the indicated temperatures using the Andrews method

Table 6 Slopes and nucleus lengths calculated from the Andrews analysis of gel fractions

Temperature (°C)	Slope	Nucleus length (Å)
107	239	302
108	256	324
109	292	370
110	251	318
111	420	532
112	391	495
113 (regime III)	438	555
113 (regime II)	102	128
115	708	899
116	741	940

the Andrews analysis has been applied only over the region in which the crosslinks are excluded (regions B and C), since it is over this defect content range that the Andrews equation applies. It should be recalled that the Andrews equation was derived assuming that the defects simply were excluded and reduced the probability of secondary nucleation without any major changes in mechanisms occurring. From the slope of the line it is possible to calculate the size of the critical nucleus. As can be seen in *Figure 13*, the slope of the line increases as the crystallization temperature is increased, meaning that the size of the critical nucleus increases with increasing crystallization temperature. This being the case, at higher crystallization temperatures the rate of nucleation would be expected to decrease since fewer chain lengths between defects would be able to participate in the nucleation step.

The slopes from *Figure 13* are listed in *Table 6* and range from 239 to 741, the values corresponding to continuous methylene units present in the critical nucleus. The values differ from the original values of Phillips and Lambert since they have been calculated over a wider range of crystallization temperatures and crosslink densities. *Table 6* includes values for the number of methylenes in the nucleus (slope) and the length of the nucleus, which is just the length of the methylene units assuming an all-*trans* configuration. The chain length of the nucleus has been used to calculate the number of stems in the nucleus. The number of stems has been calculated as the nucleus length divided by the lamellar thickness assuming a 30° tilt angle[15]. The results are shown in *Table 7*. The number of stems ranges from 0.92 to a high value of 5.6, these values being different from but including the value of 3 originally calculated by Phillips and Lambert[2]. The results suggest that in most cases the nucleus consists of multiple stems, as was suggested originally by Andrews *et al.*[6] for *cis*-polyisoprene. As pointed out by Phillips and Lambert[2], this situation may also apply to higher molecular weight polymers where chains are sufficiently long to crystallize in several lamellae simultaneously. In the case considered here, all but the two nuclei generated from the original chain ends must be composed of multiple stems. The values of the number of stems greater than 3 may be real or may be caused by the assumed 30° tilt angle, irrespective of crosslink density and crystallization temperature. The calculations also do not take into account the amount of chain used to form folds in the nucleus.

The ratio of the chain length between crosslinks to the chain length of the nucleus (*Table 7*) in most cases is <1, meaning that the nucleus cannot be formed by the average chain length between crosslinks. This does not mean that nucleation cannot occur, since a distribution of chain lengths participates in nucleation, thus making nucleation a selective process. It appears that the secondary nuclei are being formed from uninterrupted methylene sequences that are significantly greater than the average. Unfortunately, there is no acceptable method for estimating the distribution of distances between crosslinks. Several of the ratios in *Table 7* are close to 1, this being true for samples G-1.5, G-2.5 and G-3.1 at 113°C, the common regime II temperature for all three samples. The transition temperatures of G-1.5, G-2.5 and G-3.1 are 113°C, 112°C and 110°C.

Table 7 also shows that at 113°C the number of stems is equal to 1 when regime II data are used in the Andrews analysis. This suggests that the nucleation mechanism in these samples changes with the crystallization temperature and that the observed regime transition temperatures have associated with them changes in nucleation mechanism. Such a change in nucleation mechanism might involve a change from a multiple-stem to a single-stem nucleus.

The observed change in nucleation mechanism can be used to explain the regime transition in the high crosslink specimens. At low crystallization temperatures (regime III), three-stem nucleation takes place, followed by

Table 7 Nucleus shape characteristics calculated from the Andrews analysis of gel fractions

Temperature (°C)	Sample	Lamellar thickness (Å)	Number of stems	Ratio of crosslink length to nucleus length
107	G-2.5	141	1.9	0.57
	G-3.1	111	2.4	0.40
108	G-2.5	135	2.2	0.53
	G-3.1	102	3.2	0.37
109	G-1.5	119	2.7	0.53
	G-2.5	122	2.6	0.47
	G-3.1	90	3.6	0.33
110	G-1.5	114	2.4	0.62
	G-2.5	116	2.4	0.54
	G-3.1	83	3.3	0.38
111	G-0.9	150	3.1	0.61
	G-1.2	152	3.1	0.52
	G-1.5	122	3.8	0.37
	G-2.5	125	3.7	0.32
112	G-0.9	145	3.0	0.65
	G-1.2	126	3.4	0.56
	G-1.5	118	3.7	0.40
	G-2.5	114	3.8	0.35
113 (regime III)	G-0.5	175	2.8	0.94
	G-0.7	153	3.2	0.74
	G-0.9	146	3.3	0.58
	G-1.2	139	3.5	0.50
	G-1.5	121	4.0	0.35
113 (regime II)	G-1.5	121	0.92	1.21
	G-2.5	119	0.93	1.06
	G-3.1	100	1.11	0.74
115	G-0.5	165	4.7	0.58
	G-0.7	145	5.4	0.46
	G-0.9	141	5.5	0.36
	G-1.2	140	5.6	0.31
116	G-0.5	183	4.3	0.55
	G-0.7	172	4.6	0.44
	G-0.9	147	5.3	0.34
	G-1.2	139	56	0.30

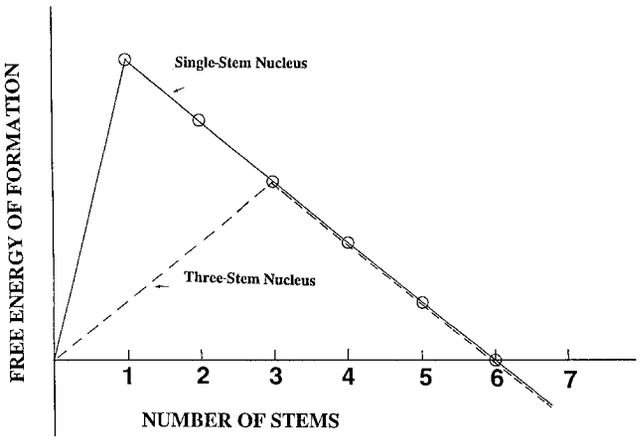

Figure 14 Schematic diagram of the free energy of stem deposition for single-stem and three-stem nuclei

limited spreading of the molecules. At higher crystallization temperatures the nucleation mechanism changes so that a single-stem nucleus is laid down and spreading can occur to a greater extent. It may be inferred from this that at higher crystallization temperatures the rate of spreading increases due to adjacent re-entry folding in addition to the noted reduction in the rate of nucleation, thus resulting in regime II growth. Again, this supports the earlier conclusion of Phillips and Lambert that the nucleation process is dependent upon the crosslink density and the crystallization temperature.

It is possible that a stable nucleus can be formed by means other than those normally considered. The free energy of formation ($\Delta\phi$) of a secondary nucleus may be given as

$$\Delta\phi = 2bl\sigma + 2ab\sigma_e - abl\Delta f$$

where a is the stem width, b is the stem thickness, l is the stem height, Δf is the free energy of crystallization and σ and σ_e are the lateral and fold surface free energy, respectively. A critical volume V^* and critical free energy $\Delta\phi^*$ can be defined as

$$V^* = a^*b^*l^* = \frac{4b^*\sigma\sigma_e}{(\Delta f)^2} \qquad \Delta\phi^* = \frac{4b^*\sigma\sigma_e}{\Delta f} = V^*\Delta f$$

Qualitatively it can be seen that changes in σ, σ_e and $\Delta f = \Delta h_f \Delta T/T_m^\circ$ will influence the dimensions of the critical nucleus. The Δh_f and T_m° can be predicted to decrease with increasing defect content from the work of Knox[19] and from the copolymer equations[14,20]. The σ_e would be expected to increase with increasing defect content as more defects are rejected to the fold surface, resulting in increased strain at the fold surface. The effect of crosslinking is to increase V^* and $\Delta\phi^*$ or, more directly, a^* and l^*.

Changes in a^* and l^* can be accommodated through changes in nucleation mechanism. An increase in l^* can occur by the laying down of longer sections of chain to form the critical nucleus. The l^* will be restricted by the chain length between defects and at some point will decrease. This means that a^* and/or b^* must increase so that V^* and $\Delta\phi^*$ may be reached, assuming they increase with crosslink density as postulated above. This suggests a change in nucleation mechanism. The possibility of 'three-dimensional' nuclei, consisting of deposition on more than one crystal plane, cannot be disregarded given the limited molecular mobility present in these crosslinked systems.

An increase in a^* can be postulated in crosslinked polyethylene through the formation of the three-stem nucleus. Nucleation in a crosslinked polymer must occur at the centre of the chain since there are no chain ends present. As the central section of the chain straightens out on the crystal face it will naturally form two constricted loops that can form two adjacent re-entry folds and ultimately generate a nucleus consisting of one complete stem and two half stems or three full stems and two folds. This was first depicted in the work of Phillips and Lambert[2]. In the case of the single-stem nucleus, which should be of higher energy than the three-stem nucleus (*Figure 14*), additional discussion is needed. This occurs in the regime II region at higher temperatures, and is the only situation encountered where the average crosslink length is close to the critical nucleus length. Presumably, it arises because of statistical probabilities being in its favour. For instance, in the case of G-1.5 (155 methylenes between crosslinks) the multiple-stem nucleus requires a length of uninterrupted methylenes three times the average number available between crosslinks. This observation suggests that the probabilities of formation of the different sizes of nuclei could be handled theoretically using a partition function approach.

It is possible to obtain additional information on the distribution of crystallinity and lamellar thickness within a specimen from determination of the height ratios and distance ratios of the uncorrected SAXS intensity curves[21]. Values obtained for these ratios are listed in *Tables 3* and *4*. The general trends observed are common to both the room temperature and *in situ* data. The height ratios tend to be the most sensitive to the distribution of crystallinity within a specimen, especially if segregation effects occur[21]. It is seen that across the series from G-0.1 to G-5.0 the height ratio decreases from 0.60–0.92 to 0.23–0.47 for the room temperature studies. This indicates a significant increase in the distribution of crystallinity within a specimen as crosslink density increases. Although there is scatter within the data, for the low crosslink density specimens there is an increase in the height ratio with crystallization temperature. This is much more clearly the case when the *in situ* results are considered. Presumably this is caused by the melting out of lamellae that were produced on cooling from the crystallization temperature. For the high crosslink density specimens, however, there appears to be little consistent change with crystallization temperature. This may be a reflection of the crystallization process being controlled by single-stem nucleation. In the studies of Jungnickel *et al.*[16,17], crystallization for crosslink densities corresponding to mole fractions of greater than 1% was said to occur in a micellar fashion. From the schematics presented in their paper, the micellar picture corresponds to the one generated here, in that it represents a near absence of adjacent re-entry folding in a lamellar system and not isolated micellar crystals. For our systems, G-1.2 and above would all have greater than 1% defect content; however, all are clearly lamellar systems from the SAXS correlation function curves, as were those of Jungnickel *et al.* Their highest crosslink density corresponded to 30 methylene units between crosslinks with a crosslink density of 30%. Our highest was 40 methylenes between crosslinks, giving manifest crystallinities of 39–51% in isothermal experiments. Hence, there do not appear to be

any major discrepancies between their data and ours; where they can be compared the agent through which crosslinking is achieved, peroxide in ours and radiation in theirs, does not appear to be a major variable. Differences may occur in the crystallization kinetics of the two types of specimen; however, such studies were not reported by Jungnickel *et al.*[16,17], so the issue must remain moot at the present time.

CONCLUSIONS

The SAXS results show that temperature has little effect on the lamellar thickness of crosslinked PE, while the chain length between crosslinks controls the lamellar thickness. The lamellar thickness variation with crosslink density combined with the crystallization kinetics shows nucleation in regime III to consist of three stems. The regime II–regime III transition is postulated to be the result of a change in nucleation mechanism from a single-stem nucleus to a three-stem nucleus.

ACKNOWLEDGEMENTS

This research was supported by the Polymers Program of the National Science Foundation under grants DMR-8719028 and DMR-9107675 awarded to the University of Tennessee. It was also supported in part by the Division of Materials Sciences, US Department of Energy, under contract DE-AC05-84OR21400 awarded to Martin Marietta Energy Systems Inc.

REFERENCES

1 Lambert, W. S. and Phillips, P. J. *Polymer* 1990, **31**, 2077
2 Phillips, P. J. and Lambert, W. S. *Macromolecules* 1990, **23**, 2075
3 Lauritzen, J. I. and Hoffman, J. D. *J. Appl. Phys.* 1973, **44**, 4340
4 Phillips, P. J. *Polym. Prepr.* 1979, **20**, 438
5 Hoffman, J. D. *Polymer* 1983, **24**, 3
6 Andrews, E. H., Owen, P. J. and Singh, A. *Proc. R. Soc. London, Ser. A* 1971, **324**, 79
7 Lambert, W. S. MS thesis, University of Tennessee, 1988
8 Hendricks, R. W. *J. Appl. Crystallogr.* 1978, **11**, 15; Wignall, G. D., Lin, J. S. and Spooner, S. *J. Appl. Crystallogr.* 1990, **23**, 241; Russell, T. P., Lin, J. S., Spooner, S. and Wignall, G. D. *J. Appl. Crystallogr.* 1988, **21**, 629
9 Lee, Y. D. PhD dissertation, University of Tennessee, 1989
10 Sanchez, I. C. and Eby, R. K. *J. Res. Nat. Bur. Stand., Sect. A* 1973, **77**, 353
11 Sanchez, I. C. and Eby, R. K. *Macromolecules* 1975, **8**, 638
12 Guiu, F. and Shadrake, L. G. *Proc. R. Soc. London, Ser. A.* 1975, **346**, 305
13 Hoffman, J. D., Davis, T. G. and Lauritzen, J. I. in 'Treatise on Solid State Chemistry' (Ed. N. B. Hannay), Vol. 3, Plenum Press, New York, 1976, p. 497
14 Flory, P. J. *Trans. Faraday Soc.* 1955, **51**, 848
15 Voigt-Martin, L. G. and Mandelkern, L. *J. Polym. Sci., Polym. Phys. Edn* 1989, **27**, 967
16 Gielenz, G. and Jungnickel, B. J. *Colloid Polym. Sci.* 1982, **260**, 742
17 Jäger, E., Müller, J. and Jungnickel, B. J. *Colloid Polym. Sci.* 1985, **71**, 145
18 Phillips, P. J. *Rep. Prog. Phys.* 1990, **53**, 549
19 Knox, J. R. in 'Analytical Calorimetry' (Eds R. S. Porter and J. F. Johnson), Vol. 1, Plenum Press, New York, 1986, p. 9
20 Flory, P. J. *J. Chem. Phys.* 1949, **17**, 223
21 Lee, Y. D., Phillips, P. J. and Lin, J. S. *J. Polym. Sci., Polym. Phys. Edn* 1991, **29**, 1235